

# Transient Performance in the Electromechanical System Network-Generator-Shaft During Asynchronous Acceleration

Arne Grüning, Stefan Kulig

Institute for Electrical Machines, Drives and Power Electronics, University of Dortmund, D-44227 Dortmund, Germany (e-mail: gruening@mal.e-technik.uni-dortmund.de, kulig@mal.e-technik.uni-dortmund.de)

**Abstract** – A 2D finite-difference time-stepping method is applied to simulate the dynamic behaviour of a turbine generator during asynchronous acceleration. The obtained simulation results, like the time functions of terminal voltages and currents, rotational speed and torque, are verified using the simulation program NETOMAC<sup>®</sup>. The applied finite-difference method further facilitates the computation of currents in specific damper bars, slot wedges and other predefined areas of the rotor body. Evaluating this results it is ascertained, that shortly after the beginning of the incident the currents in the damper winding reach very large values causing severe thermal stresses. The estimation of the temperature rise in the damper winding leads to the conclusion that already after a few seconds the acceptable temperature is exceeded and serious damages may be expected.

**Keywords** – electric machines and drives, turbine generator, asynchronous acceleration, 2D finite-difference time-stepping method, modelling decisions, thermal stresses

## I. INTRODUCTION

Faultily connecting a non excited turbine generator at low rotational speed to the transmission system leads to asynchronous acceleration of the generator, which is in that case working like an asynchronous motor. During the incident the complete shaft system has to be accelerated by the generator, which implicates the appearance of large currents in the stator windings as well as in the conductive areas of the rotor.

The main part of the currents appearing in the generator rotor is carried by the damper winding and by the massive iron near the surface in the pole region. Due to the fact that the damper winding normally is not dimensioned to sustain suchlike large currents over a longer period, damages owing to the thermal stresses due to these currents may occur.

To get a deeper understanding of the behaviour of a generator during asynchronous acceleration and especially of the currents and the thermal stresses in the conductive areas of the rotor, the asynchronous acceleration of a 170 MVA Generator is simulated by applying two methods.

A detailed simulation is carried out using the 2D finite-difference time-stepping program FELMEC, which was developed and already successfully used at the Institute for Electrical Machines, Drives and Power Electronics at the University of Dortmund. Beside the time functions of

terminal quantities, rotational speed and torque, the time functions of currents in certain areas of the rotor like slot wedges and the massive iron of the pole region as well as the distribution of the current density in the rotor at certain moments during the asynchronous acceleration are calculated. Further the simulation program facilitates a rough estimation of the temperature rise in the generator rotor using a finite-difference approach.

By examining the time functions of terminal quantities or the total time of the acceleration, an impression of the general behaviour of a generator during asynchronous acceleration can be received.

The further results are used to gain insight into the stresses especially in the generator rotor in order to estimate the possible damages caused to the generator during suchlike incident.

Afterwards a rough estimation is accomplished using the simulation program NETOMAC<sup>®</sup>. This simulation provides insight into the time behaviour of terminal currents and voltages, rotational speed and torque.

By comparing the obtained results to the corresponding results of the finite-difference simulation, the plausibility of the simulation results is surveyed.

## II. BASIC CONDITIONS

The treated bench mark shaft system consists of the 170 MVA generator with a rated terminal voltage of 13.8 kV and a gas turbine whereupon the moment of inertia of the complete shaft train amounts to about 2.5 times the moment of inertia of the generator. The generator is connected to the 110 kV transmission system by a step-up transformer.

During both simulations the field winding is simplifying assumed to be short-circuited. At the moment the asynchronous acceleration is initiated by connecting the generator to the power grid, the shaft train is stopped.

## III. FELMEC SIMULATION

The finite-difference time-stepping program FELMEC facilitates the simulation of induction machines taking into account the occurrence of eddy currents in the conductive areas of the rotor and the influence of saturation by prescribing a non-linear magnetisation curve. The usage of two separate finite-difference grids in the stator and the rotor, linked in the air gap, enables the consideration of the rotor movement [1].

By specifying terminal voltages, field voltage, mechanical torque and an initial value of rotational speed, the time behaviour of an induction machine under various transient conditions can be simulated.

#### A. Simulation Method

All quantities determined by the simulation program are based on the computation of time- and spacial-discrete magnetic vectorpotentials in the area of the generator cross section [2]. The spacial discretisation is accomplished by finite-differences using a five-point formula based on Ampere's law:

$$\oint \frac{1}{\mu} \text{rot}(A \cdot \vec{e}_z) dl = \iint -\gamma \cdot \frac{\partial(A \cdot \vec{e}_z)}{\partial t} d\vec{S} \quad (1)$$

The magnetic vectorpotential  $A_{i,k}$  in a central node  $i,k$  is calculated by applying (1) via the way  $M_1$ - $M_2$ - $M_3$ - $M_4$ - $M_1$ , as shown in Fig. 1 [1]. Occurring differential quotients are approximated by quotients of differences of the vectorpotentials of the neighbouring nodes and their distance [3].

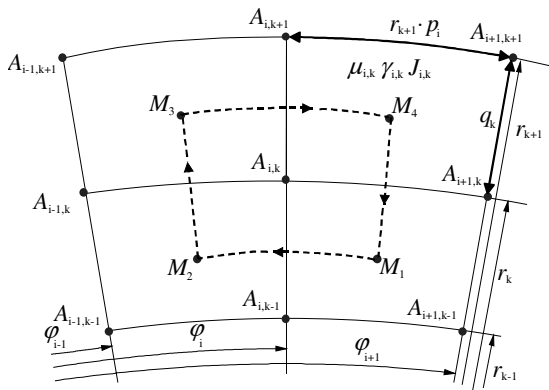


Fig. 1 Polar orthogonal finite-difference grid

In non-conductive areas of the generator cross section the right side of (1) is equal to zero. In the areas of the stator winding or the field winding the right side of (1) corresponds to the product of the current density in the respective winding, which is assumed to be constant in the winding cross section and the surface  $S$  bounded by the dashed line in Fig. 1 [4]. In other conductive areas of the generator cross section, like the massive iron of the rotor body or the slot wedges, (1) facilitates the computation of eddy currents. The time discretisation is accomplished using the  $\theta$ -method [2].

The currents in the winding cross sections and the terminal voltages are linked by circuit equations. The influence of the generator end region is emulated using lumped elements.

The movement of the rotor is determined using the motion equation. The computation of the electromagnetic torque is accomplished using an averaging evaluation of Maxwell's stress tensor for several cylindrical surfaces in the air gap [1].

The distribution of the eddy current density at certain moments during the simulation, instantaneous values of the eddy currents in predefined areas of the generator rotor and the respective power losses can be derived from the distribution of the magnetic vectorpotential.

The computation of the temperature rise in the generator rotor is accomplished using the following equation of the temperature  $\theta$ , dependent on the power losses  $q_{el}$ :

$$\oint \lambda \cdot \text{rot}(\theta \cdot \vec{e}_z) dl = \iint \left( \rho_m \cdot c_p \cdot \frac{\partial(\theta \cdot \vec{e}_z)}{\partial t} - q_{el} \cdot \vec{e}_z \right) d\vec{S} \quad (2)$$

The vector  $\theta \cdot \vec{e}_z$  is defined to enable the usage of the same mathematical routines used to compute the distribution of the magnetic vectorpotential [4]. Due to the fact that the consideration of the cooling is largely simplified, the simulation merely allows a rough estimation of the temperature rise.

#### B. Modelling and Simulation

Fig. 2 shows the finite-difference grid modelling the treated generator. The material properties are defined by the permeability  $\mu$ , including non-linear magnetisation characteristics, the conductivity  $\gamma$ , the thermal conductivity  $\lambda$ , the specific heat capacity  $c_p$  and the density  $\rho_m$ .

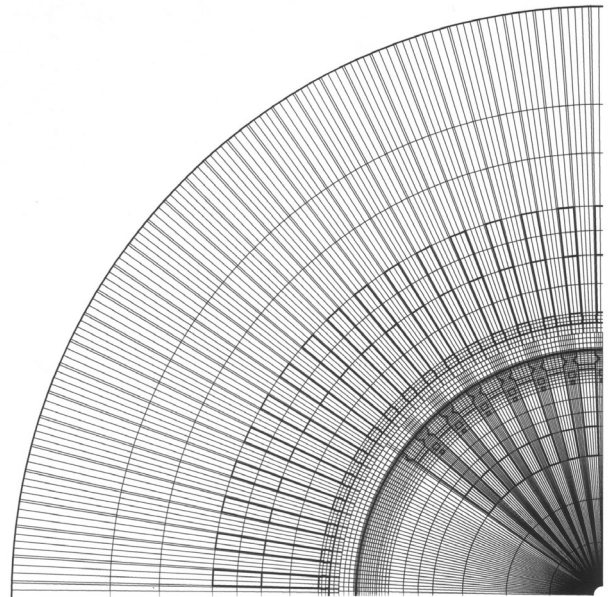


Fig. 2 Finite-difference grid modelling the generator

The model is completed by the definition of the areas of the windings in the generator cross section, the winding scheme, the lumped elements modelling the end windings, the core length of the generator and the total moment of inertia including the gas turbine. The step-up transformer is simplifying emulated by lumped elements connected to the generator terminals.

By defining the mechanical torque equal to zero the influence of friction is neglected. The cooling of the generator is roughly considered by assuming the

temperature in the air gap to be constant [4]. The initial value of the temperature is set to 20°C. The definition of the field voltage equal to zero corresponds to a short-circuited field winding.

The simulation is started with the initial value of the rotational speed set to zero and a 13.8 kV 60 Hz three-phase system connected to the generator terminals via the lumped elements emulating the step-up transformer.

#### IV. NETOMAC<sup>®</sup> SIMULATION

In order to simulate the behaviour of the generator during the asynchronous acceleration using the simulation program NETOMAC<sup>®</sup> [5], a model of the generator, the step-up transformer and the transmission system is implemented, as shown in Fig. 3. Neglecting the influence of gas friction the gas turbine is simplifying considered by replacing the moment of inertia of the generator by the moment of inertia of the complete shaft train. Other friction losses are neglected as well.

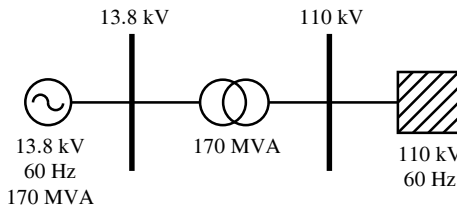


Fig. 3 Model used in simulation

The modelling of the generator is based on the Park transformation. The determination of the nominal parameters of the Park model is usually based on measurements during a three-phase terminal short-circuit. Fig. 4 shows the equivalent circuits of the d-axis and the q-axis used in the simulation. The terminals of the field voltage  $V_f$  are short-circuited.

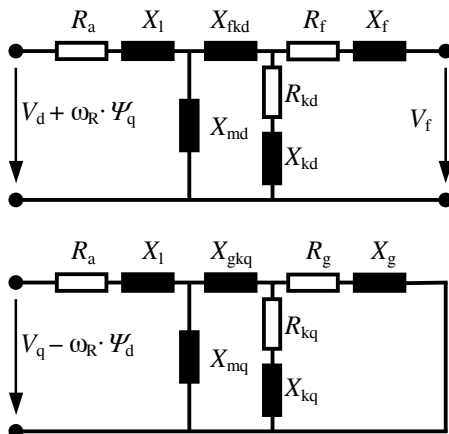


Fig. 4 Equivalent circuits of d- and q-axis

As a result of the skin effect during the asynchronous acceleration mainly the damper resistances  $R_{kd}$  and  $R_{kq}$  are dependent on rotational speed. To compensate the influence of constant damper resistances used in the NETOMAC<sup>®</sup> simulation, these resistances are multiplied by 2. To evaluate the effect of this modification two simulations are accomplished using the nominal and the modified damper resistances.

#### V. RESULTS

In the following the results of the FELMEC simulation are presented and discussed first. Afterwards the NETOMAC<sup>®</sup> results are consulted for verification purposes.

##### A. Terminal Quantities, Torque and Rotational Speed

Fig. 5 to 8 show the time functions of terminal voltage, armature current, electrical torque and rotational speed.

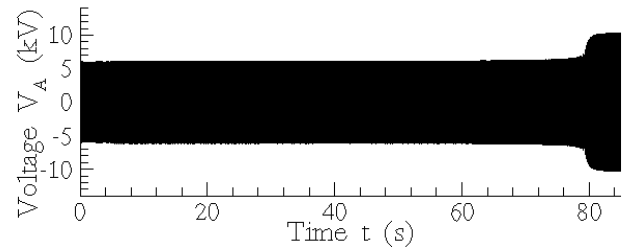


Fig. 5 Terminal voltage  $V_A$

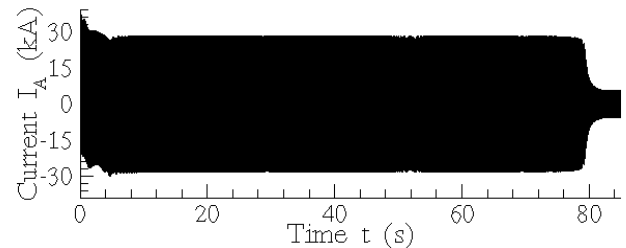


Fig. 6 Armature current  $I_A$

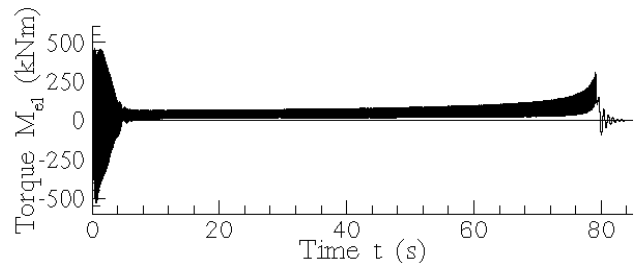


Fig. 7 Electrical torque  $M_{el}$

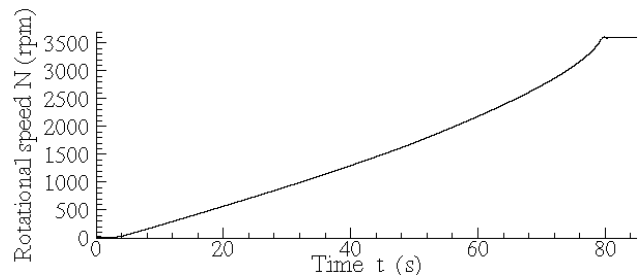


Fig. 8 Rotational speed  $N$

The total time from connecting the generator to the grid to synchronisation amounts to 80 seconds. During this time the amplitude of terminal voltage remains approximately constant. Due to the voltage drop by the transformer the effective value of the terminal voltage amounts to 4.2 kV, what corresponds to 52 % of rated voltage.

The time functions of armature current and electrical torque clearly show a transient during the first 6 seconds of the incident. Subsequently the current remains constant at

an effective value of 19.9 kA corresponding to about three times the rated current, which is in view of the duration of the incident sufficient to cause damages to the stator winding.

When the generator reaches a rotational speed of 3600 rpm, current and torque decrease within a few seconds whereas the voltage increases to nearly 90 % of rated voltage.

### B. Currents in the Generator Rotor

In the generator rotor the strains due to eddy currents are even higher. As shown in Fig. 9, the viewed areas are a slot wedge and the neighbouring tooth at the edge as well as in the middle of the field winding and further the massive iron of the pole region.

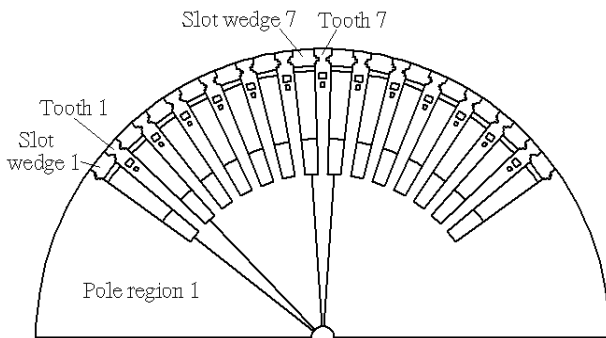


Fig. 9 Areas of eddy current computation

Fig. 10 and 11 show the time functions of the currents in slot wedge 1 and tooth 1, whereas the time functions of the currents in slot wedge 7 and tooth 7 are shown in Fig. 12 and 13.

Apart from the transient during the first 6 seconds and another transient during the synchronisation, the currents remain nearly constant during the acceleration incident. Whereas the currents in the slot wedges amount to around 40 kA, the currents in the teeth amount to merely 3 kA.

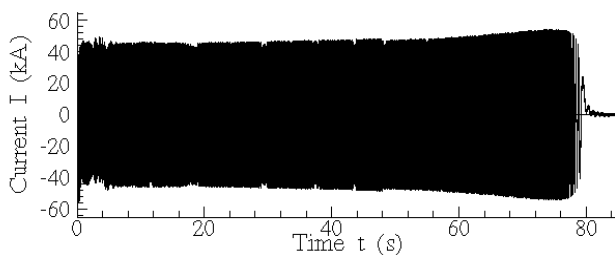


Fig. 10 Current in slot wedge 1

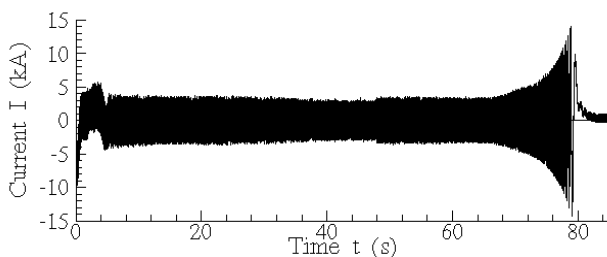


Fig. 11 Current in tooth 1

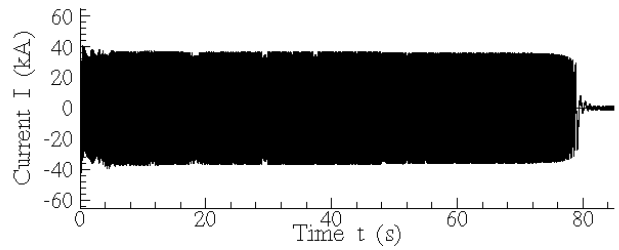


Fig. 12 Current in slot wedge 7

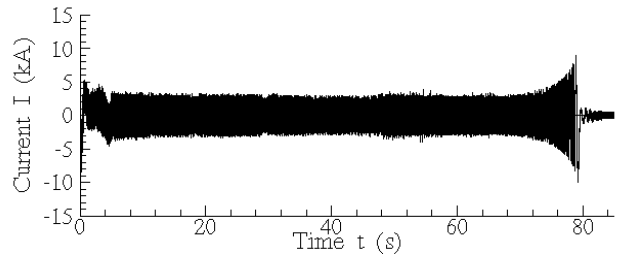


Fig. 13 Current in tooth 7

Nevertheless the power losses in both areas are comparable due to the significant lower conductivity of iron of approximately  $2.6 \cdot 10^6 \text{ Sm}^{-1}$  compared to  $2.5 \cdot 10^7 \text{ Sm}^{-1}$  of the slot wedge material. Due to the fact that the damper winding is solely designed to carry suchlike large currents during transients, damages due to thermal stresses including the softening of the material may be expected as a result of the long duration of the incident.

The time function of the current in pole region 1, shown in Fig. 14, shows characteristics comparable to the previous discussed time functions. The largeness of the current of about 140 kA follows primarily from the dimensions of the viewed area.

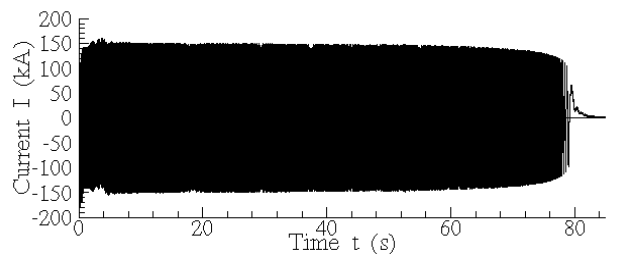


Fig. 14 Current in pole region 1

Fig. 15 shows the distribution of the current density in the rotor 2 seconds after the beginning of the incident.

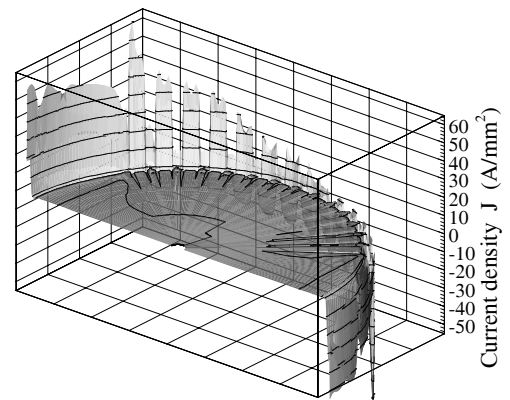


Fig. 15 Current density distribution at  $t = 2 \text{ s}$

Due to the great difference between the rotational speed of the rotor and the rotating stator field, the currents concentrate at the surface, especially in the iron areas, whereas the currents in the slot wedges spread over a slightly larger cross section.

In Fig. 16 the current density distribution at the beginning of the synchronisation is shown. As a result of the rotational speed approaching rated speed and the corresponding increase of penetration depth, the current in the field winding rises. This can also be seen in Fig. 17, showing the respective time function.

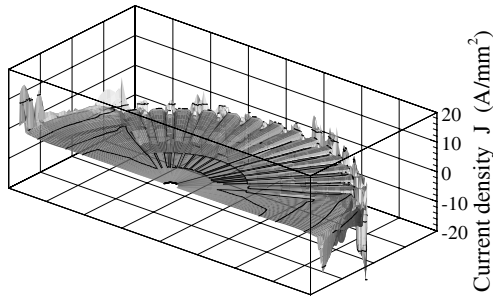


Fig. 16 Current density distribution at  $t = 79$  s

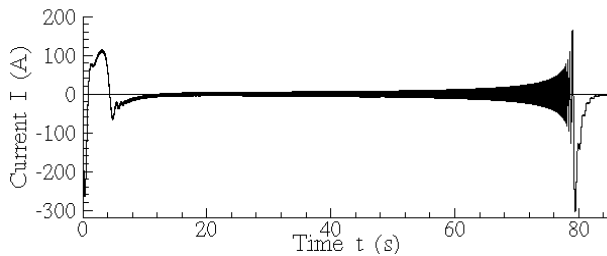


Fig. 17 Current in field winding

### C. Temperature Rise

Already after 2 seconds the temperature exceeds  $200\text{ }^{\circ}\text{C}$ , as shown in Fig. 18. The areas stressed most are the pole regions, due to the inferior thermal conductivity of the iron and the large currents concentrated close to the surface, as a result of the absence of damper bars. Inside the slot wedges the thermal conduction is observably higher.

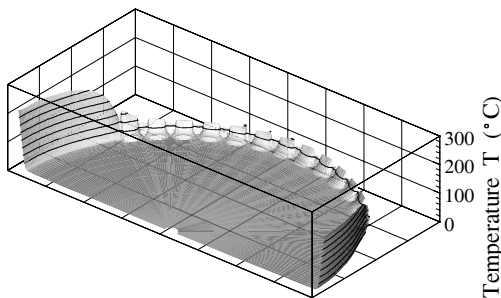


Fig. 18 Temperature distribution at  $t = 2$  s

After 17 seconds the calculated temperature reaches values around  $1000\text{ }^{\circ}\text{C}$ , as shown in Fig. 19. Although the simulation method allows merely a rough estimation of the temperature rise, it can be ascertained that after a noticeable shorter time than the duration of the complete incident, temperatures sufficient to cause softening of the material are reached.

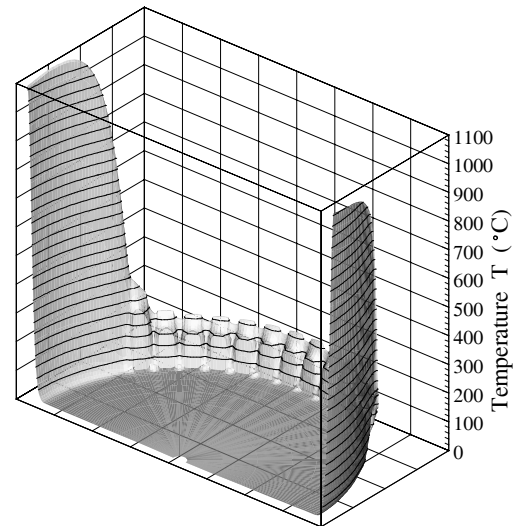


Fig. 19 Temperature distribution at  $t = 17$  s

### D. Comparison to NETOMAC® Results

Fig. 20 and 21 show the comparison of terminal voltage and armature current computed using FELMEC to the corresponding results of the two accomplished NETOMAC® simulations.

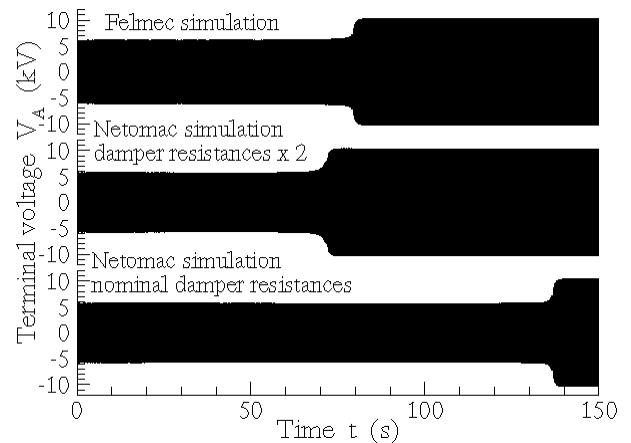


Fig. 20 Comparison of terminal voltage  $V_A$

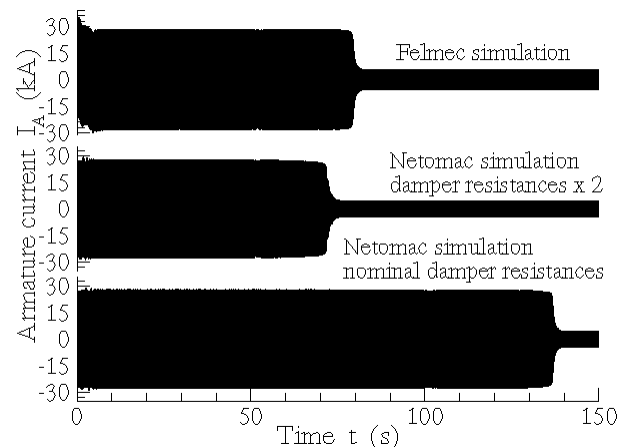


Fig. 21 Comparison of armature current  $I_A$

Apart from the transient directly after the beginning of the incident, the difference between the diagrammed results

regarding the amplitude is mostly less than 5 %. Merely the current after synchronisation computed using FELMEC is nearly 25 % larger than in the NETOMAC<sup>®</sup> results. This can be ascribed to the definition of constant parameters of the Park model, which only facilitates a rough consideration of the influence of saturation. The appearance of the DC component during the first transient in the current of phase A in the FELMEC results and not in the NETOMAC<sup>®</sup> results follows from different moments of connecting the generator to the grid.

The comparison of electrical torque and rotational speed computed using FELMEC to the corresponding results of the two accomplished NETOMAC<sup>®</sup> simulations is shown in Fig. 22 and 23. Using the nominal parameters of the equivalent circuits, NETOMAC<sup>®</sup> computes a significant longer duration of the acceleration incident of around 136 seconds.

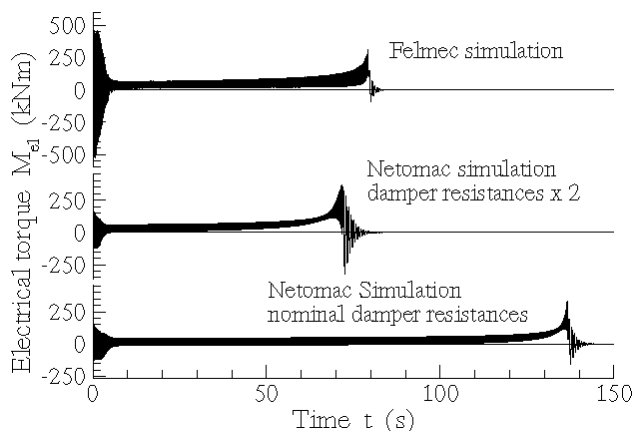


Fig. 22 Comparison of electrical torque  $M_{el}$

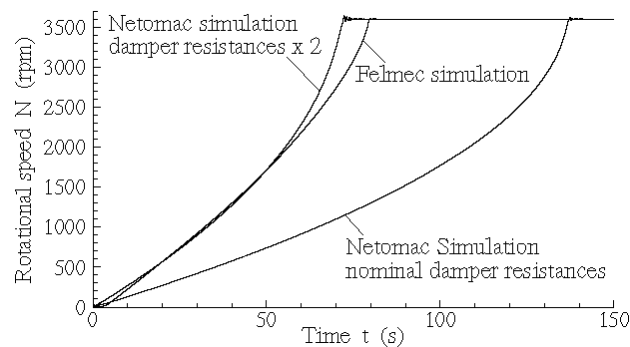


Fig. 23 Comparison of rotational speed  $N$

Due to the fact that the electrical torque is proportional to the power losses in the generator rotor, taking not into

account the influence of the skin effect by using constant damper resistances leads to an unprecise computation of the electrical torque. As a result of this the increase of rotational speed is calculated significant lower. Multiplying the damper resistances by 2, a duration of the incident of around 72 seconds is calculated.

To achieve more precise results in simulating an asynchronous acceleration the influence of saturation and the skin effect have to be considered, like it is done when using the 2D finite-difference time-stepping method. Applying a simulation method based on the Park transformation requires the modification of the damper resistances  $R_{kd}$  and  $R_{kq}$ . As shown in Fig. 20 to 23 the accomplished modification of the damper resistances is sufficient to obtain a rough estimation.

## VI. CONCLUSIONS

During the asynchronous acceleration the thermal stresses due to the eddy currents in the generator rotor are high to such an extent that already after a few seconds severe damages may be expected. Further the large armature currents are sufficient to cause damages to the stator winding.

The precise simulation of an asynchronous acceleration requires the consideration of the skin effect and the influence of saturation. Applying simulation methods based on the Park transformation, a modification of the damper resistances enables the accomplishment of a rough estimation.

## REFERENCES

- [1] R. Gottkehasch, "Nichtlineare Berechnung von Asynchronmaschinen mit massiveisernem Rotor und zusätzlichem Käfig im transienten Zustand mittels Finiter Differenzen und Zeitschrittrechnung, dissertation," VDI-Verlag, Düsseldorf, 1993.
- [2] R. Ummelmann, "Erweiterung eines Finite-Differenzen-Zeitschritt-Programmsystems auf Synchronmaschinen, diploma thesis," Institute for Electrical Machines, Drives and Power Electronics, University of Dortmund, 1997.
- [3] M. Klocke, "Determination of Dynamical Phenomena in Soft-Started Induction-Motor-Devices Using the Finite-Difference Time-Stepping Method," ISEF'99, Pavia, pp. 185-190, 1999.
- [4] O. Drubel, "Elektromagnetische Vorgänge und Temperaturverteilungen im Rotor großer Turbogeneratoren im gestörten Betrieb, dissertation," VDI-Verlag, Düsseldorf, 2001.
- [5] B. Kulicke, "Simulation von Drehfeldmaschinen mit beliebigen Ersatzschaltungen," Siemens Forschungs- und Entwicklungsberichte, Vol. 12, 1983.